Acta Oceanol. Sin., 2017, Vol. 36, No. 9, P. 52–64
DOI: 10.1007/s13131-017-1111-2
http://www.hyxb.org.cn
E-mail: hyxbe@263.net

Geochemical and microbial characters of sediment from the gas hydrate area in the Taixinan Basin, South China Sea

GONG Junli[1], SUN Xiaoming[1, 2, 3*], LIN Zhiyong[1], LU Hongfeng[4], LU Yongjun[5]

[1] School of Earth Science and Engineering, Sun Yat-sen University, Guangzhou 510275, China

[2] School of Marine Sciences, Sun Yat-sen University, Guangzhou 510006, China

[3] Guangdong Provincial Key Laboratory of Marine Resources and Coastal Engineering, Guangzhou 510006, China

[4] Guangzhou Marine Geology Survey, Guangzhou 510075, China

[5] School of Life Sciences, Sun Yat-sen University, Guangzhou 510275, China

Received 2 September 2016; accepted 6 December 2016

Abstract

The Taixinan Basin is one of the most potential gas hydrate bearing areas in the South China Sea and abundant gas hydrates have been discovered during expedition in 2013. In this study, geochemical and microbial methods are combinedly used to characterize the sediments from a shallow piston Core DH_CL_11 (gas hydrate free) and a gas hydrate-bearing drilling Core GMGS2-16 in this basin. Geochemical analyses indicate that anaerobic oxidation of methane (AOM) which is speculated to be linked to the ongoing gas hydrate dissociation is taking place in Core DH_CL_11 at deep. For Core GMGS2-16, AOM related to past episodes of methane seepage are suggested to dominate during its diagenetic process; while the relatively enriched δ^{18}O bulk-sediment values indicate that methane involved in AOM might be released from the "episodic dissociation" of gas hydrate. Microbial analyses indicate that the predominant phyla in the bacterial communities are Firmicutes and Proteobacteria (Gammaproteobacteria and Epsilonproteobacteria), while the dominant taxa in the archaeal communities are Marine_Benthic_Group_B (MBGB), Halobacteria, Thermoplasmata, Methanobacteria, Methanomicrobia, Group C3 and MCG. Under parallel experimental operations, comparable dominant members (Firmicutes and MBGB) are found in the piston Core DH_CL_11 and the near surface layer of the long drilling Core GMGS2-16. Moreover, these members have been found predominant in other known gas hydrate bearing cores, and the dominant of MBGB has even been found significantly related to gas hydrate occurrence. Therefore, a high possibility for the existing of gas hydrate underlying Core DH_CL_11 is inferred, which is consistent with the geochemical analyses. In all, combined geochemical and microbiological analyses are more informative in characterizing sediments from gas hydrate-associated areas in the South China Sea.

Key words: Geochemistry, Microbial community, 16S rRNA, Gas hydrate, Taixinan Basin, South China Sea

Citation: Gong Junli, Sun Xiaoming, Lin Zhiyong, Lu Hongfeng, Lu Yongjun. 2017. Geochemical and microbial characters of sediment from the gas hydrate area in the Taixinan Basin, South China Sea. Acta Oceanologica Sinica, 36(9): 52–64, doi: 10.1007/s13131-017-1111-2

1 Introduction

Gas hydrate is an ice-like crystalline substance, composed of cages that are predominantly consisted of water and nature gas (Kvenvolden, 1993). It occurs both in polar region and offshore deep-water marine sediments under appropriate conditions including low temperature, high-pressure as well as adequate methane concentrations (Lu et al., 2007). Owing to its high potential for being an alternative energy resource (Kvenvolden, 1988), increasing attentions have been attracted into studying gas hydrate recently. Among these, much more efforts have been put into finding evidences that can indicate the occurrence of gas hydrate (Lu et al., 2015; Zhang et al., 2014a).

Geochemical analysis is a commonly used method in gas hydrate investigation. Changes in pore water chlorinity concentration as well as δ^{18}O and δD value with depth are conclusive evidences for the presence of gas hydrate (Hesse, 2003; Kvenvolden and Kastner, 1990). In addition, obviously decreasing variation in pore water sulfate concentration (Borowski et al., 1996, 1999; Dickens, 2001; Tréhu et al., 2004; Yang et al., 2008, 2010), strong depleted δ^{13}C value of pore water dissolved inorganic carbon (DIC) or authigenic carbonates in sediments (Campbell, 2006; Han et al., 2008; Lu et al., 2005, 2006; Yang et al., 2008), as well as the changing contents of redox-sensitive trace elements (Helz et al., 1996, 2011; Hu et al., 2014, 2015; McManus et al., 2006; Sato et al., 2012; Zheng et al., 2000, 2002), are also suggested to be linked to the presence of deep buried gas hydrate (e.g., Bhatnagar et al., 2008; Borowski et al., 1996; Niewöhner et al., 1998). This is owing to an upward flux of methane that fuels anaerobic oxidation of methane (AOM), during which sulfate is reduced by methane with 1:1 stoichiometry and the isotope features as well as the redox state of the ambient sediment or pore water are also changed correspondingly (Lin et al., 2016a, b, 2017). The overall

Foundation item: The Natural Science Foundation of China under contract Nos 91128101, 41273054 and 41373007; the China Geological Survey Project for South China Sea Gas Hydrate Resource Exploration under contract No. DD20160211; the Fundamental Research Funds for the Central Universities under contract No. 16lgjc11; the Guangdong Province Universities and Colleges Pearl River Scholar Funded Scheme under contract No. 2011.

*Corresponding author, E-mail: eessxm@mail.sysu.edu.cn

reaction of AOM is represented as following:

$$CH_4 + SO_4^{2-} \rightarrow HCO_3^- + HS^- + H_2O. \quad (1)$$

Alternatively, studies have also suggested that there is potential specialization of microbial communities in gas hydrate as well as related sedimentary niches (Inagaki et al., 2006; Jiao et al., 2015; Mills et al., 2003; Yanagawa et al., 2014). Through comparison analyses, studies found that the dominant microbial taxa in hydrate-containing areas differ with that in the hydrate-free sediments (Inagaki et al., 2006; Jiao et al., 2015; Yanagawa et al., 2014). It is also suggested that the dominance of JS1 and Marine_Benthic_Group_B (MBGB) are significantly related to the occurrence of gas hydrates (Parkes et al., 2014). These demonstrate that special microbial communities, though often not unequivocal, might be used as complementary indicators for identifying gas hydrate occurrence. So far, consistent constraints from both geochemical and microbial analyses regarding to the occurrence of gas hydrate in the South China Sea (SCS) have been rarely documented.

In this study, geochemistry and 16S rRNA gene phylogenetic analyses are integrated used to study the sediments from a shallow piston Core DH_CL_11 and a hydrate-bearing Core GMGS2-16. Our scientific interests are:

(1) characterizing the geochemical and microbiological features of the two cores;

(2) exploring the main biogeochemical process occurs in the two cores;

(3) exploring the possible relationships between the aforementioned features and process with gas hydrate occurrence.

2 Method

2.1 *Site description and sampling*

The SCS is one of the largest marginal seas of the western Pacific, located at the conjunction region of the Eurasian Plate, the Pacific Plate and the Indian Plate (Lu et al., 2011). The two study sites are located in the Taixinan Basin (Fig. 1), which is in the direction of northeast (NE), with a length of about 400 km, average width of 150 km, a water depth of 200–3 500 m, and an area of more than 60 000 km^2 (He et al., 2006). Two depressions respectively distribute in the north and the south of this basin, separated by an uplift in the NE direction. The thickness of the Cenozoic sediments in the depressions can reach 8 000 m, and the thickness of the sediments in the eastern part of the basin can reach 7 000 m offshore Kaohsiung, which provide suitable pressure-temperature regime to form and host gas hydrate (McDonnell et al., 2000). Tectonically, the evolution of the Taixinan Basin can be divided into three periods: rifting (eventually caused the formation of the basin), compression (developed a lot of reverse faults and related folds) and thermal subsidence (generated horizontal sediment layers which are basically not controlled by the effects of faulting) (Ding et al., 2004).

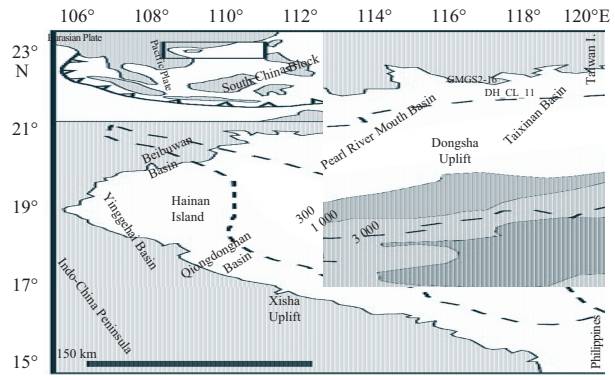

Fig. 1. Sketch map showing the locations of sedimentary basins in the northern South China Sea (modified from Sun et al. (2012)). The black dots mark the sites of Cores DH_CL_11 and GMGS2-16, which are located within the Taixinan Basin. Inset (top left): regional setting.

Various types of seafloor morphologies, such as the abyssal trough, undersea cliffs, ocean plateau, steep slope, valley, sea slide and submarine fan, are common observed in this basin (Lu et al., 2011; Yang et al., 2010). Fault-fold system, diapirs and gravity flow deposits are also widely distributed (Chen et al., 2006). These provide favorable geological settings and structures for gas hydrate formation. Heat flow data in the Taixinan Basin subseabed are highly variable. A much higher heat flows had been found just above the mud diapirs, showing that deep fluid migration occurred there (Shyu et al., 1998). Strong bottom-simulating reflectors (BSRs), generally interpreted to be related to the occurrence of gas hydrate, have been reported existed in this basin, demonstrating its potential for the occurrence of gas hydrate (e.g., Li et al., 2013; McDonnell et al., 2000; Song et al., 2001; Shyu et al., 2006; Wu et al., 2005). Meanwhile, Structure I gas hydrates characterized by shallow burying, thick layers, multiple types and high saturation have been discovered in this basin in 2013 (Zhang et al., 2014a).

The two studied sediment cores (DH_CL_11 and GMGS2-16) were collected during HY4-2012-06 and GMGS2 cruises. Core DH_CL_11 (21°56′N, 118°53′E) was collected by gravity piston, is about 767 centimeters long and showed a strong smell of hydrogen sulfide gas during onboard sampling. This core is located in one of the three gas hydrate prospect areas in the south and west of Taiwan (McDonnell et al., 2000), and vast area of seep carbonates called “Jiulong Methane Reef” has ever been reported in its immediate vicinity (Li et al., 2013). Estimated thickness of the gas hydrate stability zone under Core DH_CL_11 is around 280 m (Bi, 2010). GMGS2-16 is one of the gas hydrate-bearing cores recovered from voyage GMGS2, which is about 235 meters long and located on the boundary between the Zhujiang River Mouth Basin and the Taixinan Basin (Zhang et al., 2014a). Double hydrate horizons were identified in this core, with nodular hydrates presenting at 15–30 mbsf (meters below seafloor) and fine vein-like hydrates presenting at 189–226 mbsf.

Sediment subsamples were collected from each sediment core. For molecular analyses, three samples (CL_11_2, CL_11_11 and CL_11_35) from Core DH_CL_11 and four samples (16_1, 16_13, 16_15 and 16_39) from Core GMGS2-16 were selected. The corresponding sampling depth of each sample is marked in Fig. 2 by dash lines. Upon retrieving, samples were carefully peeled and the inner part of each sample were frozen at –20°C until analyses.

2.2 *Geochemical analysis*

Total organic carbon (TOC) and total sulfur (TS) in sediments were determined with an Elementar Vario EL Cube CHNOS analyzer in the Instrumental Analysis and Research Center of Sun Yat-sen University (Guangzhou) according to the procedures described in Freire et al. (2012). Briefly, sediment samples were firstly powdered and treated using 10% HCl solution to remove carbonate, rinsed with distilled water, and then dried in the oven until analysis. Carbon- and O-isotope ratios

were measured on a Finnigan MAT 252 mass spectrometer. The CO_2 used for $\delta^{13}C$ and $\delta^{18}O$ measurements was extracted from the carbonate component of the bulk sediment with pure H_3PO_4 at 75°C. All data are reported relative to the PDB standard. Headspace methane content was analyzed on board, following the operation procedures and methods described by Yin et al. (2011). Pore water sulfate concentration was measured using ion chromatography (Metrohm790IC), and the standard deviation from repeated measurement of sulfate content in standard sea water was less than 2%.

The SMI (sulfate-methane interface) depth was calculated by Linear Regression. Fick's First Law was used to calculate the flux of sulfate:

$$F = -\emptyset D_{\text{sed}} \cdot \frac{\partial C}{\partial x}, \tag{2}$$

in marine sediment:

$$D_{\text{sed}} = \frac{D_{\text{sw}}}{1 + n(1 - \emptyset)}, \tag{3}$$

where F is the flux, $\emptyset$ is porosity, $\partial C/\partial x$ is the concentration gradient, D_{sed} and D_{sw} are the free-solution diffusion coefficient in marine sediments and sea water, respectively. Here, the assessed D_{sw}, porosity, n value are inherited from Wu et al. (2013), which are 0.55×10^{-9} m^2/s, 68.39% and 3, respectively. The flux of sulfate can be calculated out by Eqs (2) and (3).

2.3 *Nucleic acid extraction and purification*

DNA was extracted from 0.5 g sediments using the E.Z.N.A Soil DNA kit (OMEGA, USA) according to the instruction of the manufacturer. Duplicated DNA extractions were combined before purification through gel extraction (AXYGEN, USA). The concentration was quantified in duplicate using BioTek Epoch (USA). The total volume of the elution buffer was 80 μl.

2.4 *Pyrosequencing*

Bacterial and archaeal 16S rRNA genes covering the V1-V3 and V3-V5 regions were selected to construct community libraries through tag-encoded 454 pyrosequencing. Amplicon pyrosequencing was performed using a 454/Roche A sequencing primer kit on a Roche Genome Sequencer GS-FLX Titanium platform at Majorbio Bio-Pharm Technology Co., Ltd., Shanghai, China. After pre-experimenting, the minimum number of thermal cycles was set to 25 and 33 for the bacterial and archaeal community analyses, respectively. The thermal cycling scheme used for the amplification of the partial bacterial 16S rRNA genes was as follows: initial denaturation at 95°C for 2 min, 25 cycles of denaturation at 95°C for 30 s, annealing at 55°C for 30 s, extension at 72°C for 30 s, and final extension period at 72°C for 5 min. The thermal cycling scheme used for the amplification of the partial archaeal 16S rRNA genes was as follows: initial denaturation at 95°C for 2 min, 33 cycles of denaturation at 95°C for 30 s, annealing at 53°C for 30 s, extension at 72°C for 30 s, and final extension period at 72°C for 5 min. Negative controls contained the entire reaction mixture without the template DNA.

2.5 *Phylogenetic analysis*

The filtered sequences were trimmed using the trimseq script from the EMBOSS package (Rice et al., 2000). The average length of the edited reads for bacterial and archaeal community are 252 and 256 bp, respectively. These reads were aligned with the bacterial and archaea SILVA (SSU111) database (http://www.arb-silva.de) using "align.seqs" commands (http://www.mothur.org/wiki/Align.seqs). UCHIME (http://drive5.com/uchime) was used to determine chimeric sequences. Furthest neighbor commands were used and unique sequences were clustered into operational taxonomic units (OTUs) defined by 97% similarity. For taxonomic classification, sequences with identity scores greater than 97% identity (<3% divergence) to known or well characterized 16S rRNA sequences were resolved at the species level, between 95% and 97% at the genus level, between 90% and 95% at the family, between 85% and 90% at the order, 80%–85% at the class, 70%–80% at phyla (Stackebrandt and Goebel, 1994). The data preprocessing and OTU-based analysis were performed on Mothur Win.

2.6 *Nucleotide sequences accession number*

All 454-GS Junior sequence data in this study were submitted to the NCBI Sequence Read Archive (SRA) under accession number SRP072268.

3 Results

3.1 *Geochemical features*

The TOC of sediments from the DH_CL_11 and GMGS2-16 ranges from 0.53% to 1.26% and 0.51% to 1.15%, respectively. The TS of sediments from both sites are 0.04% to 0.40% and 0.02% to 0.75%, respectively. On the depth profile of Core DH_CL_11, the TS show an increasing variation trend. It increases steadily from 0.04% at 20 cmbsf (centimeters below seafloor) to 0.15% at 707 cmbsf, and then sharply increases to 0.40% at 747 cmbsf. The TS in core GMGS2-16 illustrates a fluctuating trend, with multiple layers having the maximum TS values (Figs 2b and f).

The stable C, O isotopes of bulk sediment carbonates was analyzed. The $\delta^{13}C$ and $\delta^{18}O$ values of sediments from Core DH_CL_11 range from –1.9‰ to –0.2‰ and –4.2‰ to –1.7‰, respectively, and those of core GMGS2-16 range from –12.1‰ to 0.4‰ and –8.2‰ to –0.7‰, respectively (Figs 2c and g). On the depth profile of Core DH_CL_11, the variation trends of the $\delta^{13}C$ and $\delta^{18}O$ values opposite to each other. The $\delta^{13}C$ values generally decreases with depth. While the $\delta^{18}O$ values increases from –4.2‰ in the near surface layer to –1.7‰ at around 500 cmbsf, and then slight decreases to –2.3‰ or –2.4‰. The $\delta^{13}C$ and $\delta^{18}O$ values of Core GMGS2-16 illustrate a fluctuating trend, but the contrasting changing trends between the $\delta^{13}C$ and $\delta^{18}O$ values still persists.

Pore-water sulfate concentration and the methane content in headspace gases from Core DH_CL_11 were also detected. Generally, the sulfate concentration displays a decrease pattern along the depth profile. Methane contents above 650 cmbsf are only at a much lower level, but a dramatic increase is documented at 700 cmbsf (Fig. 2d).

3.2 *Microbial features*

3.2.1 *Overview of pyrosequencing*

Bacterial and archaeal 16S rRNA gene (SSU) amplicons prepared from seven sediment samples were analyzed. Fourteen pyrosequencing dataset containing 7,077–19,524 sequences were generated with an average length range between 350 and 600 bases (Table 1). The number of OTUs (at 97% similarity level) detected across the two sampling cores ranges from 130 to 1 541, and 36 to 1 114 in the bacterial and archaeal communities, respectively. The richness and diversity index of microbial com-

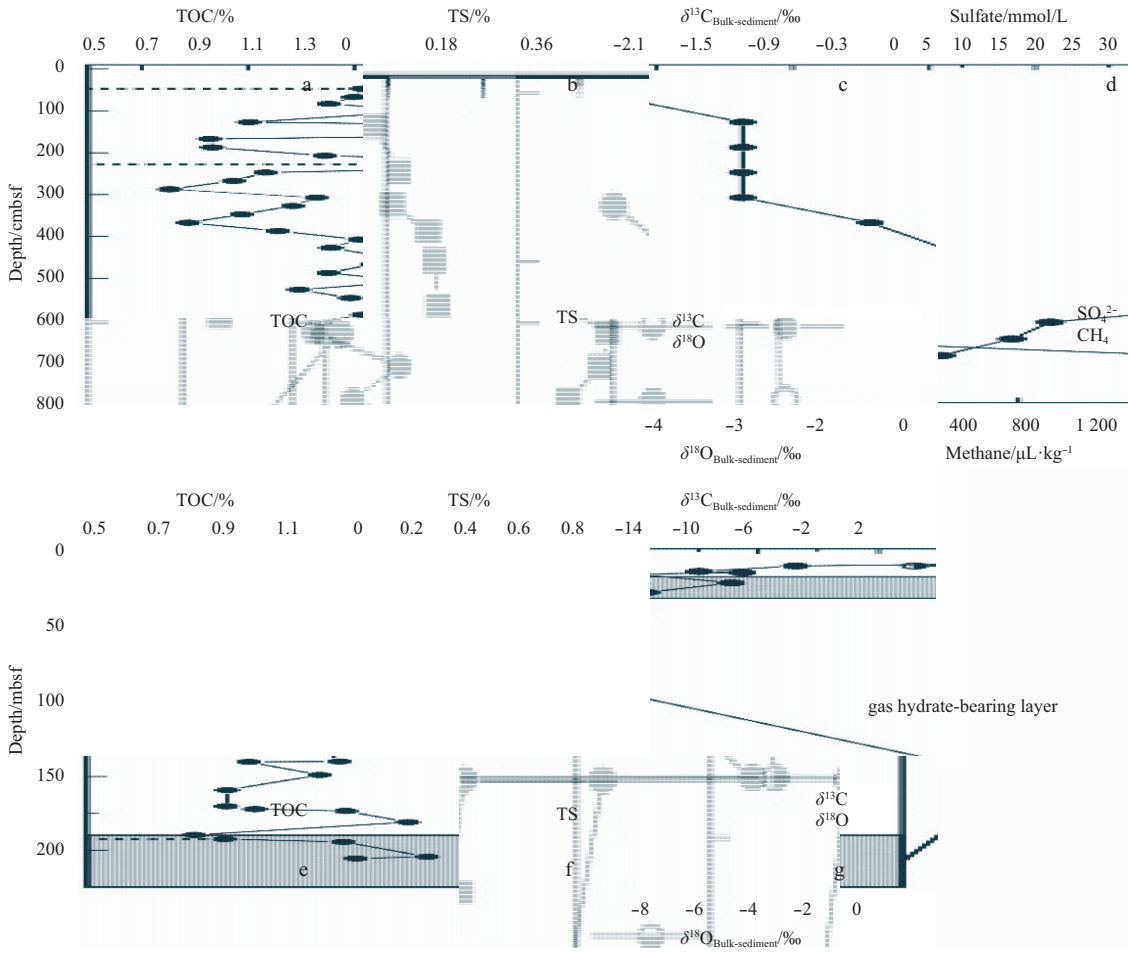

Fig. 2. Depth profiles of geochemical parameters in core DH_CL_11 and core GMGS2-16 (dash lines mark the sampling layers).

Table 1. Diversity indexes, including OTU, ACE, Chao1, Coverage, Shannon, and Simpson, of bacterial and archaeal 16S rRNA genes

Sample ID	Depth/mbsf	Reads	97% similarity level					
			OTU	ACE[a]	Chao1[b]	Coverage[c]	Shannon[d]	Simpson[e]
B_CL_11_2	0.47	11 031	1 541	7 457	4 237	0.904 2	3.62	0.197 5
B_CL_11_11	2.27	11 300	1 397	6 068	3 460	0.917 0	3.49	0.202 1
B_CL_11_35	7.07	12 058	1 412	5 874	3 368	0.923 2	3.43	0.211 8
B_16_1	0.15	18 725	264	280	277	0.998 2	2.60	0.274 7
B_16_13	18.15	19 524	152	170	171	0.998 6	1.64	0.489 3
B_16_15	24.65	17 831	103	120	115	0.998 8	1.02	0.659 2
B_16_39	192.35	19 081	131	141	139	0.999 2	2.12	0.340 3
A_CL_11_2	47	7 077	783	1 265	1 251	0.961 3	5.61	0.010 5
A_CL_11_11	227	8 787	1 114	1 934	1 743	0.949 4	5.74	0.010 0
A_CL_11_35	707	7 868	480	1 092	842	0.976 2	4.79	0.025 7
A_16_1	0.15	12 520	134	137	137	0.999 3	2.48	0.168 5
A_16_13	18.15	12 988	64	71	82	0.999 3	2.25	0.179 1
A_16_15	24.65	7 276	36	36	36	0.999 9	2.30	0.145 0
A_16_39	192.35	7 230	44	46	46	0.999 6	2.97	0.073 9

Note: [a]: Nonparametric statistical prediction of the total OTUs based on the distributions of abundant and rare OTUs; [b]: Nonparametric statistical prediction of the total OTUs based on the distributions of singletons and doubletons; [c]: Coverage $=[1-(n_1/N)]\times 100$, where n_1 is the number of unique OTUs, and N is the total number of clones in a library; [d]: A higher number indicates greater diversity; [e]: A lower number indicates greater diversity.

munity structure were summarized in Table 1. The coverage rates in the bacterial and archaeal community range from 0.904 2 to 0.999 9, demonstrating that the majority of the phylotypes had been covered by surveying effort. Comparative analysis indicated that, as a whole, the microbial richness of the shallow piston core (DH_CL_11) was much higher than that of the gas hydrate-bearing core (GMGS2-16). Similar, the richness of archaea was also higher in Core DH_CL_11.

3.2.2 *Taxonomic composition*

Firmicutes and Proteobacteria are the most predominant members in the bacterial community (Fig. 3a). The former accounts for a large proportion (80.65%–92.48%) in samples from core DH_CL_11 as well as the near seafloor sample (16_1) from core GMGS2-16. The latter account for a significant part (81.29%–93.26%) of the bacterial communities of the other three layers from core GMGS2-16. Other phylum or groups, like Actinobacteria, Bacteroidetes, Candidate_division_OP8, Chloroflexi, Planctomycetes and Spirochaetae are also frequently detected in the bacterial communities, and each of them account for at least 0.5% of the bacterial community.

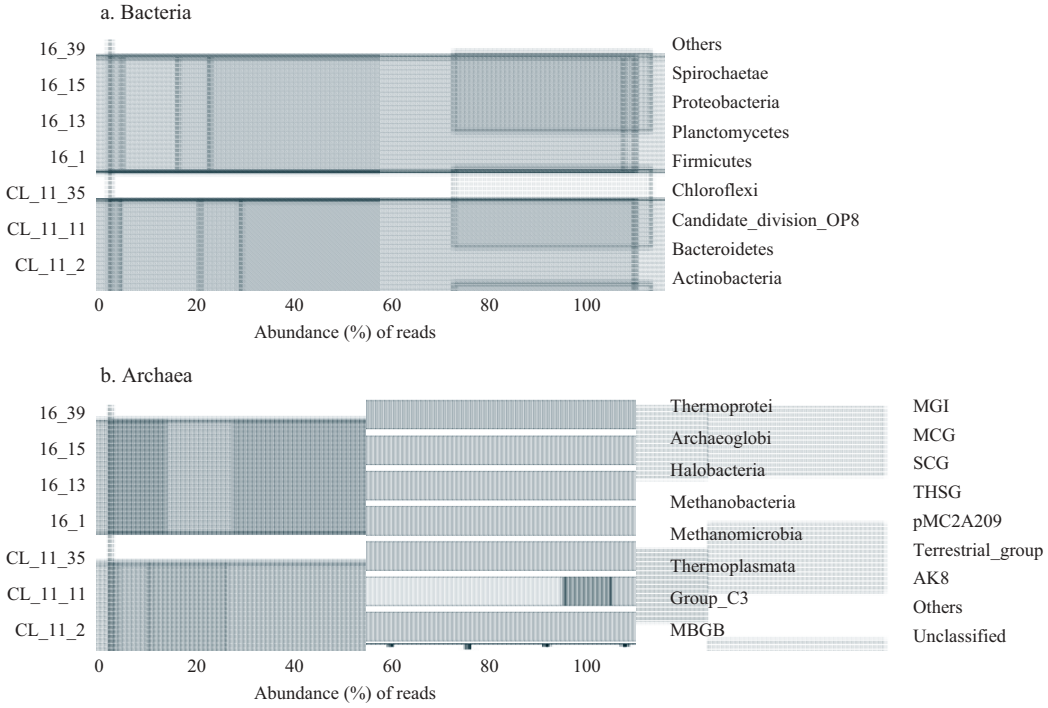

Fig. 3. Phylogenetic community compositions based on 16S rRNA gene sequences. a. Bacteria and b. Archaea.

A detailed phylogenetic analysis of the top 20 OTUs of each community were conducted (Table 2). From it we can see, 16/20 of the OTUs in Core DH_CL_11 are assigned to *Lactococcus*, whichalso account for a large portion of the top 20 OTUs from sample 16_1. Ectothiorhodospiraceae, a family belonging to Gammaproteobacteria, has the largest sequence numbers in the bacterial community of core GMGS2-16. These sequences are mainly assigned to sample 16_13 and 16_15. *Sulfurimonas*, a genus belonging to Helicobacteraceae in Epsilonproteobacteria, has the third largest number, sequences of which are originally from sample 16_39.

For the archaeal community, the dominant members in each sample are different (Fig. 3B). Halobacteria and Thermoplasmata are highly abundant in CL_11_2 and CL_11_11. Sequences belonging to Halobacteria are mainly assigned to Deep Sea Hydrothermal Vent Group-6 (DSHVGp-6) (Table 3). Lineages within Thermoplasmata are mainly assigned to Marine_Benthic_Group_D (MBGD), South Africa Gold Mine Archaea-R (SAGMA-R) and South Africa Gold Mine Archaea-I (SAGMA-I) (Table 3). MBGB are predominant in all detected archaeal communities but that of 16_39. MCG were generally frequently detected (3.36%–11.09%) in all chosen samples, while MGI were only detected abundantly in CL_11_2 (13.03%) and CL_11_35 (15.48%). Group C3 were abundantly detected (17.70%) in sample 16_15. Methanobacteria and Methanomicrobia are the dominant archaeal class in 16_39, accounting for 20.57% and 40.53% of the detected community, respectively. Besides, Methanomicrobia also represented 39.98% of the detected archaeal members in 16_13. Lineages assigned to class Methanomicrobia and Methanobacteria at the genus or family level mainly consist of *Methermicoccus*, *Methanosarcina*, *Methanosaeta*, *Methanobacterium*, Methanomicrobiaceae and ANME-1b, with most of them being methanogens except for ANME-1b (Table 3).

4 Discussion

4.1 *Indications from the geochemical parameters*

TOC in marine sediments are residual carbon survived seafloor and shallow subseafloor diagenesis (Johnson et al., 2014). Those preserved below the sulfate reduction zone in marine sediments could be used as substrates for methanogenesis (Johnson et al., 2014). The TOC contents in the studied sediment cores (0.51%–1.26%) are in the range of that in the surface sediments from the Taixinan Basin (0.04%–1.37%), and they have reached the threshold (0.4%–0.5%) for *in situ* biogenic gas hydrate formation (Klauda and Sandler, 2005; Waseda, 1988). However, the inconsistency variation trends between the headspace methane and TOC in Core DH_CL_11 suggest that the sharply increasing methane at the bottom layer is not generated by methanogenesis *in situ* but originally come from deep.

The total sulfur in sediments comprises organic sulfur and inorganic sulfur (e.g., sulfate, sulfide). On the depth profile of Core DH_CL_11, the pore water sulfate concentration decreases gradually, TS show an increasing trend, and only a weakly correlation exists between the TS and TOC. These demonstrate that inorganic sulfur, specially the sulfide, is the main component of the total sulfur in sediments. TOC/TS keep decreasing with depth,

Table 2. The top 20 bacterial OTUs in different samples from Cores DH_CL_11 and GMGS2-16

Rank	Total	CL_11_2	CL_11_11	CL_11_35	Phyium	Class	Order	Family	Genus
#1	14 797	4 673	4 835	5 289	Firmicutes	Bacilli	Lactobacillales	Streptococcaceae	*Lactococcus*
#2	3 472	1 121	1 141	1 210	Firmicutes	Bacilli	Lactobacillales	Streptococcaceae	*Lactococcus*
#3	2 978	898	982	1 098	Firmicutes	Bacilli	Lactobacillales	Streptococcaceae	*Lactococcus*
#4	444	145	138	161	Firmicutes	Bacilli	Lactobacillales	Streptococcaceae	*Lactococcus*
#5	405	124	129	152	Firmicutes	Bacilli	Lactobacillales	Streptococcaceae	*Lactococcus*
#6	386	127	124	135	Firmicutes	Bacilli	Lactobacillales	Carnobacteriaceae	*Carnobacterium*
#7	367	102	124	141	Firmicutes	Bacilli	Lactobacillales	Streptococcaceae	*Streptococcus*
#8	362	138	147	77	Firmicutes	Bacilli	Lactobacillales	Streptococcaceae	*Lactococcus*
#9	260	78	92	90	Firmicutes	Bacilli	Lactobacillales	Streptococcaceae	*Lactococcus*
#10	236	73	83	80	Firmicutes	Bacilli	Lactobacillales	Streptococcaceae	*Lactococcus*
#11	196	39	85	72	Firmicutes	Bacilli	Lactobacillales	Streptococcaceae	*Lactococcus*
#12	195	85	49	61	Firmicutes	Bacilli	Lactobacillales	Streptococcaceae	*Lactococcus*
#13	185	9	146	30	Actinobacteria	Actinobacteria	no_rank_Actinobacteria	Nocardiaceae	*Rhodococcus*
#14	181	52	64	65	Firmicutes	Bacilli	Lactobacillales	Streptococcaceae	*Lactococcus*
#15	178	70	54	54	Firmicutes	Bacilli	Lactobacillales	Streptococcaceae	*Lactococcus*
#16	169	52	44	73	Firmicutes	Bacilli	Lactobacillales	Streptococcaceae	*Lactococcus*
#17	163	48	66	49	Firmicutes	Bacilli	Lactobacillales	Streptococcaceae	*Lactococcus*
#18	145	43	46	56	Firmicutes	Bacilli	Lactobacillales	Streptococcaceae	*Streptococcus*
#19	116	38	35	43	Firmicutes	Bacilli	Lactobacillales	Streptococcaceae	*Lactococcus*
#20	96	39	13	44	Firmicutes	Bacilli	Lactobacillales	Streptococcaceae	*Lactococcus*

Rank	Total	16_1	16_13	16_15	16_39	Phylum	Class	Order	Family	Genus
#1	28 004	35	13 544	14 425	0	Proteobacteria	Gammaproteobacteria	Chromatiales	Ectothiorhodospiraceae	
#2	12 939	9 646	1 339	275	1 679	Firmicutes	Bacilli	Lactobacillales	Streptococcaceae	*Lactococcus*
#3	10 887	1	4	31	10 851	Proteobacteria	Epsilonproteobacteria	Campylobacterales	Helicobacteraceae	*Sulfurimonas*
#4	1 762	4	134	26	1 598	Proteobacteria	Alphaproteobacteria	Rhodobacterales	Rhodobacteraceae	–
#5	1 695	1	817	877	0	Proteobacteria	Gammaproteobacteria	Chromatiales	Ectothiorhodospiraceae	–
#6	1 226	1 008	76	18	124	Firmicutes	Bacilli	Lactobacillales	Streptococcaceae	*Lactococcus*
#7	945	2	423	520	0	Proteobacteria	Gammaproteobacteria	Oceanospirillales	Alcanivoracaceae	*Alcanivorax*
#8	925	704	91	16	114	Firmicutes	Bacilli	Lactobacillales	Streptococcaceae	*Lactococcus*
#9	866	716	63	10	77	Firmicutes	Bacilli	Bacillales	Bacillaceae	*Bacillus*
#10	640	15	3	580	42	Bacteroidetes	Flavobacteria	Flavobacteriales	Flavobacteriaceae	*Muricauda*
#11	583	394	70	17	102	Firmicutes	Bacilli	Lactobacillales	Streptococcaceae	*Lactococcus*
#12	561	468	35	2	56	Actinobacteria	Actinobacteria	Micrococcales	Micrococcaceae	*Arthrobacter*
#13	529	5	337	17	170	Proteobacteria	Alphaproteobacteria	Rhodobacterales	Rhodobacteraceae	*Roseovarius*
#14	510	282	3	2	223	Bacteroidetes	Flavobacteria	Flavobacteriales	Flavobacteriaceae	*Muricauda*
#15	507	310	85	1	111	Proteobacteria	Gammaproteobacteria	Alteromonadales	Alteromonadaceae	*Marinobacter*
#16	468	0	15	0	453	Proteobacteria	Gammaproteobacteria	Thiotrichales	Piscirickettsiaceae	–
#17	420	328	31	6	55	Firmicutes	Bacilli	Lactobacillales	Streptococcaceae	*Lactococcus*
#18	416	356	24	2	34	Firmicutes	Bacilli	Bacillales	Planococcaceae	*Lysinibacillus*
#19	378	0	339	39	0	Proteobacteria	Gammaproteobacteria	Oceanospirillales	Alcanivoracaceae	*Kangiella*
#20	363	0	14	7	342	Proteobacteria	Alphaproteobacteria	Rhodobacterales	Rhodobacteraceae	*Thioclava*

Table 3. The top 20 archaeal OTUs in different samples from Cores DH_CL_11 and GMGS2-16

Rank	Total	CL_11_2	CL_11_11	CL_11_35	Phylum	Class	Order	Family	Genus
#1	1 703	407	382	914	Thaumarchaeota	MBGB			
#2	985	243	288	454	Thaumarchaeota	MBGB			
#3	548	9	166	373	Euryarchaeota	Thermoplasmata	SAGMA-R		
#4	515	302	205	8	Thaumarchaeota	MCG			
#5	487	2	450	35	Euryarchaeota	Thermoplasmata	MBGD		
#6	427	259	126	42	Thaumarchaeota	MBGB			
#7	417	14	90	313	Euryarchaeota	Thermoplasmata			
#8	299	0	0	299	Euryarchaeota	Thermoplasmata	SAGMA-I		
#9	270	2	58	210	Euryarchaeota	Thermoplasmata	SAGMA-R		
#10	251	104	133	14	Euryarchaeota	Thermoplasmata	MBGD		
#11	221	49	172	0	Euryarchaeota	Thermoplasmata	MBGD		
#12	191	22	78	91	Thaumarchaeota	MBGB			
#13	183	13	160	10	Euryarchaeota	Thermoplasmata	MBGD		
#14	166	61	29	76	Thaumarchaeota	pPACMA-Y			
#15	165	36	118	11	Euryarchaeota	Thermoplasmata	MBGD		
#16	137	7	44	86	Euryarchaeota	Thermoplasmata	MBGD		
#17	137	17	106	14	Thaumarchaeota	THSGp			
#18	131	50	27	54	Thaumarchaeota	MBGB			
#19	120	86	16	18	Thaumarchaeota	MBGB			
#20	120	0	120	0	Euryarchaeota	Halobacteria	DSHVGp-6		

Rank	Total	16_1	16_13	16_15	16_39	Phylum	Class	Order	Family	Genus
#1	7 125	2 588	2 312	2 125	100	Thaumarchaeota	MBGB			
#2	6 889	3 718	1 940	1 113	118	Thaumarchaeota	MBGB			
#3	4 238	34	4 202	2	0	Euryarchaeota	Methanomicrobia	Methanosarcinales	Methermicoccaceae	*Methermicoccus*
#4	2 815	18	1 687	700	410	Thaumarchaeota	MBGB			
#5	2 559	2 151	151	256	1	Thaumarchaeota	MBGB			
#6	1 382	53	405	722	202	Thaumarchaeota	MCG			
#7	1 248	16	106	16	1 110	Euryarchaeota	Methanomicrobia	Methanosarcinales	Methanosarcinaceae	*Methanosarcina*
#8	1 036	0	0	0	1 036	Euryarchaeota	Methanomicrobia	Methanosarcinales	Methanosaetaceae	*Methanosaeta*
#9	884	626	138	4	116	Thaumarchaeota	MBGB			
#10	726	0	0	0	726	Euryarchaeota	Methanobacteria	Methanobacteriales	Methanobacteriaceae	*Methanobacterium*
#11	723	723	0	0	0	Thaumarchaeota	MCG			
#12	556	30	7	519	0	Thaumarchaeota	Group_C3			
#13	509	478	19	12	0	Thaumarchaeota	MBGB			
#14	507	0	507	0	0	Euryarchaeota	Methanomicrobia	Methanomicrobiales	Methanomicrobiaceae	
#15	482	0	3	479	0	Thaumarchaeota	AK8			
#16	474	31	0	443	0	Thaumarchaeota	Group_C3			
#17	419	0	0	0	419	Euryarchaeota	Methanobacteria	Methanobacteriales	Methanobacteriaceae	*Methanobacterium*
#18	393	0	0	0	393	Euryarchaeota	Methanomicrobia	ANME-1	ANME-1b	
#19	379	3	187	86	103	Thaumarchaeota	MBGB			
#20	372	118	70	169	15	Thaumarchaeota	MBGB			

with TOC/TS from the bottom part being lower than that of the normal marine sediments (2.8±0.8) (Zhang et al., 2015) (Fig. 4a). This indicates that extra sulfur, which is not generated from sulfate reduction by TOC, contributes to the sulfur pool at the bottom part. The significant correlation between the TS and the headspace methane suggests that upward methane from deep is the main cause of the increasing TS in sediments. Therefore, we proposed that the sharply elevated TS are affected by AOM.

In Core GMGS2-16, many layers have the maximum TS values, which roughly correspond to layers with lower TOC/TS values than the normal marine sediments (the shadow area) (Fig. 4b). Generally, there is a positive correlation between TS and TOC contents, with an average TS/TOC ratio of 0.36 in "oxic-suboxic marine sediments" (Berner, 1982; Sato et al., 2012). A nearly constant TS/TOC ratio always turns out at non-seep sediments with oxic seawater, while sediments from the "cold seep" sites do not follow this correlation owing to the hydrogen sulfide generated during AOM (Goldhaber, 2003). In this study, high TS/TOC ratios, ranging from 0.03 to 1.35 and falling out of non-seep marine sediment facies, are observed in core GMGS2-16. Three anomalous TS/TOC areas (in dashed circle), which are consistent well with layers having TOC/TS lower than 2.8±0.8, are delineated (Fig. 4c). These suggest that ancient AOM processes had repeatedly occurred during its sedimentary history.

AOM has been described to play an important role in influencing the pore-water sulfate concentration and gradient in methane-rich sediments, and it has also suggested to be linked to the presence of deep buried gas hydrate (e.g., Bhatnagar et al., 2008; Borowski et al., 1996; Niewöhner et al., 1998). It occurs within the seafloor sediments, where pore water sulfate, meet methane from methanogenesis and/or thermogenesis zones (Freire et al., 2012). That interface is named sulfate-methane interface (SMI), where SO_4^{2-} and CH_4 are consumed to zero concentrations at significantly high rate (Boetius et al., 2000). The calculated SMI depth in Core DH_CL_11 is 8.6 mbsf, which is comparable to other adjacent cores characterized by high methane flux from the same basin (Lu et al., 2011). Such depth is even lower than that in the gas hydrate bearing area from Blake Ridge (Borowski et al., 1999), falling into a range of the SMIs from the gas hydrate occurrence areas worldwide. The SO_4^{2-} flux in Core DH_CL_11 is 23.19 mmol/m^{2}a, close to the upper limit (26.9 mmol/m^{2}a) of that from the Shenhu area of SCS and slightly higher than in the gas hydrate area at the Blake Ridge (8.2–18 mmol/m^{2}a) (Borowski et al., 1996). Such shallow SMI depth, high sulfate flux as well as the sharply elevated headspace methane concentration suggests high methane flux in this core. As for the source of methane, it could be migrated from a gas hydrate decomposing layer or other types of deep gas source (Ye et al., 2016)

For core GMGS2-16, a trend of increasing TS observed at 0–3 mbsf is similar to that in the Core DH_CL_11 (Fig. 5b). Considering that Core DH_CL_11 is affected by the high methane flux and that there is a shallow buried gas hydrate-bearing layer (15–30 mbsf) in core GMGS2-16, we suppose that the increase of TS, resulting from AOM, might be related to the underlying gas hydrate dissociation. In addition, bicarbonate released during AOM, which could result in a noticeable increase in alkalinity at the SMI depth (Nauhaus et al., 2005). High alkalinity is beneficial to precipitation of authigenic carbonates (Boetius et al., 2000; Jørgensen et al., 2004; Snyder et al., 2007), if there is enough Ca^{2+}, Mg^{2+} in the ambient pore water. In the current study, the $\delta^{13}C_{bulk\text{-}sediment}$ value in Core DH_CL_11 ranges from –1.9‰ to –0.2‰, close to that of the marine carbonates, suggesting that normal marine carbonates are the major components in carbonate rocks. This is consistent with our microscope observation that biological carbonates appeared in large numbers in sediments (data not shown). A decreasing trend in $\delta^{13}C_{bulk\text{-}sediment}$ values was observed on the depth profile, similar to the trend of $\delta^{13}C_{DIC}$ in this core (Ye et al., 2016). Relative depleted $\delta^{13}C_{bulk\text{-}sediment}$ values occurred near the inferred SMI, comparable with that in the adjacent piston cores GC10 and HD319 reported by Lu et al. (2011). This suggests that the gradually depleted $\delta^{13}C_{bulk\text{-}sediment}$ values are related to AOM, and that AOM is ubiquitous in sediment cores characterized by high methane flux in the Taixinan Basin. Contrast to $\delta^{13}C_{bulk\text{-}sediment}$, the $\delta^{18}O_{bulk\text{-}sediment}$ shows an increasing trend with depth, with relative $\delta^{18}O$-rich values at the ^{13}C-depleted zone (Fig. 2c). Compared to the seep carbonates samples acquired from the vicinity area (Han et al., 2008, 2013, 2014), these $\delta^{18}O_{bulk\text{-}sediment}$ values are much closer to that of the normal marine carbonates. However, it seems unlikely that such a regular trend is due to an internal random fluctuation. Thus, an

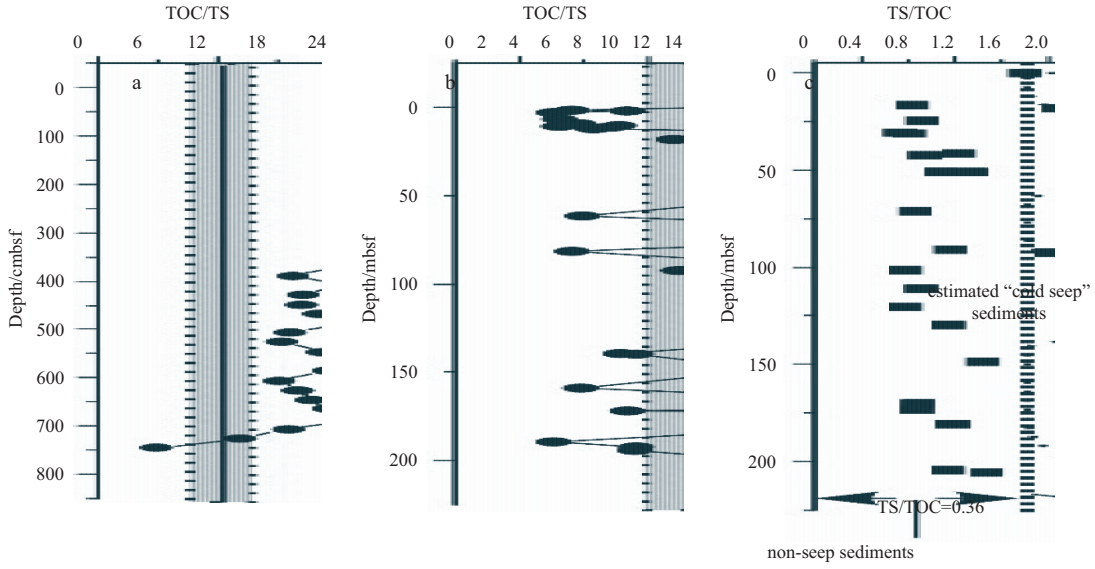

Fig. 4. Depth profiles of TOC/TS in Core DH_CL_11 (a) and Core GMGS2-16 (b), as well as the TS/TOC in Core GMGS2-16 (c).

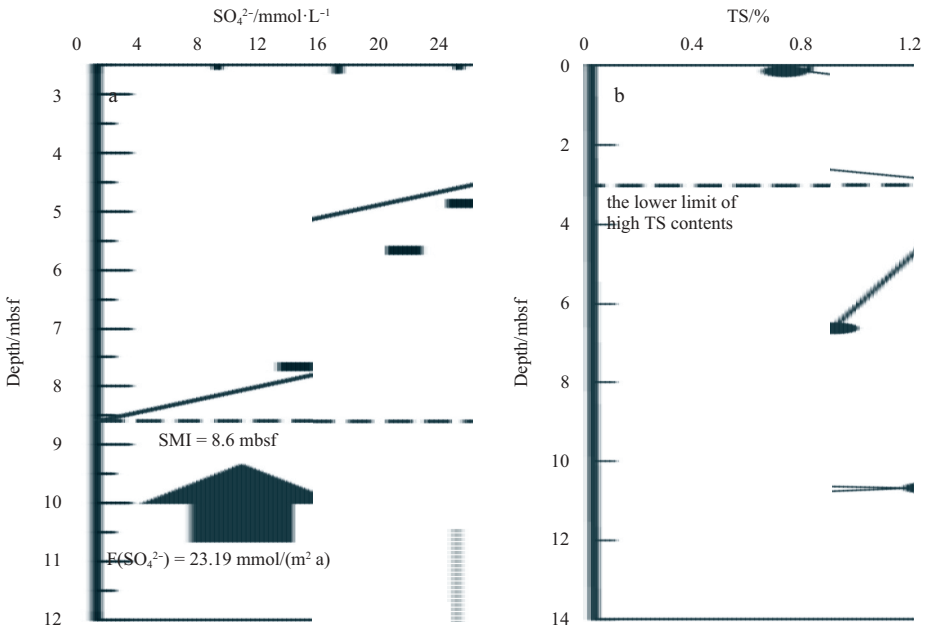

Fig. 5. Diagram of SMI depth and flux of sulfate for core DH_CL_11 (a) and the TS variation trend above the gas hydrate-bearing layer of in core GMGS2-16 (b).

ascending fluids enriched in ^{18}O from deep sea are suggested to influence this sediment core. Generally, ancient seawater, water from gas hydrate decomposition and clay mineral dehydration are the main sources of $\delta^{18}O$-rich fluids (Dählmann and de Lange, 2003; Pierre et al., 2000; Takeuchi et al., 2002). Until now, the dehydration of clay mineral in large-scale in this basin has not been reported yet (Lu et al., 2011). Besides, it is unlikely that the ancient seawater is a main factor because of the opposite changing trend between $\delta^{18}O$ and $\delta^{13}C$. Therefore, the best explanation of the $\delta^{18}O$ values in Core DH_CL_11 should be that it has been influenced by fluids from gas hydrate dissociation. Moreover, the pore water salinity at the lower part of Core DH_CL_11 decreased with depth, which furtherly supported that gas hydrate is dissociating underlying (Gong et al., 2014). This interpretation is only tentative, and more persuasive evidences are needed to indicate the occurrence of underlying gas hydrate.

In Core GMGS2-16, the ^{13}C-depleted and ^{18}O-enriched values of bulk sediment turn up intermittently along the depth profile, which can be attributed to the occurrence of the authigenic seep carbonates in these depths (unpublished data). These indicate that intense AOM appeared intermittently, which is generally interpreted as a response to the "episodic dissociation" of gas hydrate. Such an interpretation has been drawn from other neighboring gas hydrate bearing cores in this area. For example, Chen et al. (2016) suggested that at least 6 episodes of gas hydrate release existed in the geologic record of Core GMGS2-08, and that the varying sizes of authigenic carbonate among the layers are indicators of different intensity of methane flux in each episode. Zhuang et al. (2016) suggested that the integrated ^{13}C-depleted and ^{18}O-enriched values of foraminifera in sediment core are important evidences for the occurrence of gas hydrate decomposition during sedimentary history. Thus, we conclude that the gas hydrate reservoirs in this area have been running a circulation of accumulation, release and re-accumulation. Aerobic oxidation, anaerobic oxidation, released into the seawater/atmosphere, or staying in the sediment core are the possible fates of methane from gas hydrate decomposition. While, from the point of view of a long geological history, it seems that the gas hydrate in one sediment core is undergoing a cycling of decomposition, migration and re-storage.

The crossplot of $\delta^{13}C$ versus $\delta^{18}O$ is useful to differentiate seep ($\delta^{13}C$-depleted and $\delta^{18}O$-rich) from normal marine (non-seep) sediments. In this study, sediments from DH_CL_11 and GMGS2-16 plot closely with another two hydrate potential cores in the Taixinan Basin (Lu et al., 2011). Some of these data are shifting to sediments from the Hydrate Ridge (Wang and Suess, 2002), but most of the data are still separated from them (Fig. 6). The possible reason for this may be owing to the existence of large amount of biological carbonates in the sediment cores and few carbonates from AOM. However, the opposite changing trends of the $\delta^{13}C$ and $\delta^{18}O$ values on the depth profiles has demonstrated that AOM has happened or/and is happening in our studied cores.

4.2 *Indications from the microbial community analyses*

The predominance (80.65%–92.48%) of the Firmicutes group in the shallow sediments (including all three layers from the shal-

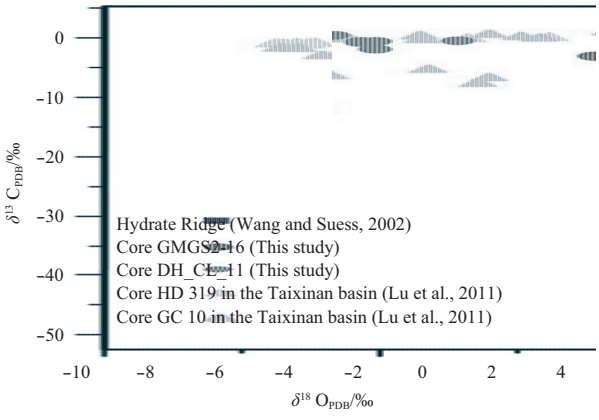

Fig. 6. The $\delta^{13}C$ versus $\delta^{18}O$ of sediments in the South China Sea.

low piston core and the near surface layer from Core GMGS2-16) is one of the prominent features observed in the bacterial diversity. Compared to the microbial-investigating studies that have been conducted in sediments from the SCS (Table 4), the dominant microbial groups in this study are quite different from that in the surface sediments of northern/southern slope (Liao et al., 2009; Li et al., 2008a), Xisha Trough (Li et al., 2008b) and the Qiongdongnan Basin (Jiang et al., 2007). This indicates that the distribution of microbial community varies under different geographic location. Nevertheless, the dominant bacterial phyla in Core DH_CL_11 and a cold seep site from the same basin also differ with each other (Zhang et al., 2012). This indicates that other factors aside from geographic location affected the acquired microbial community. Besides, shared dominant groups cannot be observed in the gas hydrate-bearing Core GMGS2-16 and the gas hydrate-bearing cores from the Shenhu area, indicating that the presence of hydrate presence or not might not be the controlling factor for the microbial distribution in hydrate-containing sediments (Jiao et al., 2015). Consistent conclusion can also be drawn from the microbial diversity analyses conducted in worldwide gas hydrate-existing or related areas (e.g., Boetius and Suess, 2004; Briggs et al., 2012, 2013; Jiao et al., 2015; Lanoil et al., 2005; Nunoura et al., 2012; Yan et al., 2006; Zhang et al., 2012), in which the dominant members are always quite variable among different areas.

Parkes et al. (2014) proposed that the choice of different "universal" bacterial or archaeal-specific PCR primer/probe for 16S rRNA genes can add biases into the microbial community structure analyses (Parkes et al., 2014). It reminds us of the need of caution in comparing microbial communities between different studies. Adding that the distribution of microbial community varies under different geographic location, we proposed that valid comparison is limited to geographical proximity as well as parallel experimental operations. For example, results from the comparative analyses of the microbial communities in hydrate-containing and hydrate-free cores from geographically close sites revealed dominant members in the two kinds of isolation places different with each other (Jiao et al., 2015; Inagaki et al., 2006; Yanagawa et al., 2014). These actually verify that the geographic location and especially the parallel experimental operations may play an important role in distinguishing different niches. In this study, under parallel experimental operations, shared predominant taxa——Firmicutes and MBGB, are observed in samples from the piston core (DH_CL_11) and the near surface layer of the gas hydrate-bearing drilling core (GMGS2-16). Therefore, a high possibility for the existing of gas hydrate underlying Core DH_CL_11 is inferred, which is consistent with the geochemical analyses.

Firmicutes have been abundantly detected in a crude oil-impacted gas hydrate-bearing site (Station 156) from the Gulf of Mexico (Orcutt et al., 2010), a deep layer of Site UBGH2-10 from the Ulleung Basin (Lee et al., 2013), as well as a long hydrate-bearing drilling core (Site 17A) from the Andaman Sea (Briggs et al., 2012). Besides, Phylotypes within this phylum are commonly abundantly detected in deep oil or coal deposits, such as the crude oil deposits in Japan, oil field in Malaysian and subsurface coal beds from Canada (Li et al., 2012; Penner et al., 2010; Yamane et al., 2011). Firmicutes have been reported as major decomposers of organic matter in biogas reactors (Tang et al., 2005). These members are mainly involved in hydrolyzing complex organic compounds and converting them to oligomers and monomers which can be utilized directly by methanogenic Archaea or further degraded by the so-called secondary fermenting bacteria (Kampmann et al., 2012). Thus, it is reasonable that Firmicutes can be dominant in gas hydrate-containing environment, since intense methanogenesis usually carried out at depth (Marchesi et al., 2001). This also helps to explain why the dominance of Firmicutes only occurs at a deep layer of Site UBGH2-10 from the Ulleung Basin. However, previous research pointed out that Firmicutes could be transported by wind over short or long distances (Polymenakou and Mandalakis, 2013). Therefore, they can be abundantly detected in any layers of a sediment core.

As for MBGB, the predominant of MBGB has been reported in many gas hydrate-related areas, such as the hydrate zones in the Nankai Trough (Reed et al., 2002), the Sea of Okhotsk (Inagaki et al., 2003a), the Ulleung Basin (Briggs et al., 2013; Lee et al., 2013) and the "cold seep" area from the Taixinan Basin. Besides, by statistical analysis, the dominant MBGB has been found significantly correlated with the occurrence of gas hydrates (Parkes et al., 2014). Thus, the predominant of MBGB in most of the detected subsections in this study might also be related with a gas hydrate system, but its specific relationship to gas hydrates is still not clear.

In summary, conditional comparison results of the dominant members between DH_CL_11 and GMGS2-16, and the abundant distribution of Firmicutes and MBGB in other gas hydrate-bearing cores both suggest that there might be gas hydrate buried at depth of Core DH_CL_11. However, it is noteworthy that the dominant bacterial/archaeal phylogroups detected here are mainly involved in organic matter decomposition (*Lactococcus* in Firmicutes) (Schleifer et al., 1985), sulfur-oxidation (Ectothi-

Table 4. Comparative analyses of the microbial communities in sediments from the South China Sea

Isolation environment	Dominant Bacteria	Dominant Archaea	Reference
Surface sediments of Northern slope of South China Sea	Gammaproteobacteria Deltaproteobacteria Planctomycetes	MGI	(Liao et al., 2009)
Surface sediments of Southern slope of South China Sea	Deltaproteobacteria Planctomycetes Acidobacteria	MBGB; MGI; MBGD; SAGMEG	(Li et al., 2008a)
Xisha Trough	Alphaproteobacteria Deltaproteobacteria Planctomycetes	MGI; TMEG	(Li et al., 2008b)
Shenhu area without gas hydrate	Planctomycetes	MBGD	(Jiao et al., 2015)
Qiongdongnan Basin	Gammaproteobacteria Alphaproteobacteria Deltaproteobacteria Firmicutes	MBGB; MCG	(Jiang et al., 2007)
Cold seep in Taixinan Basin	Chloroflexi JS1	MBGB; Group C3; MBGD; Halobacteriales	(Zhang et al. 2012)
DH_CL_11 in Taixinan Basin	Firmicutes	MBGB; Halobacteria; Thermoplasmata (MBGD)	This study
GMGS2-16 in Taixinan Basin	Firmicutes Gammaproteobacteria Epsilonproteobacteria	MBGB; Group C3; Methanomicrobia; Methanobacteria	This study

orhodospiraceae in Gammproteobacteria and *Sulfurimonas* in Epsilonproteobacteria) (Inagaki et al., 2003b); Tourova et al., 2007), and methane generation (lineages within Methanomicrobia and Methanobacteria). While, very few sequences are related to known sulfate reduction bacteria (SRB) and ANME, although a coupled biogeochemical process including sulfate reduction and AOM is expected to exist in both Cores DH_CL_11 and GMGS2-16. Since AOM mainly occurs in the sulfate methane transition zone (SMTZ) (Harrison et al., 2009; Knittel and Boetius, 2009; Reeburgh, 2007), a possible explanation for this phenomenon might be that we fail to choose layers characterized by typical SMI features. Meanwhile, the chosen of different PCR primers for 16S rRNA genes may further aggravate this bias.

5 Conclusion

In this study, we analyzed the geochemical and microbial characters of sediments from a shallow piston core in a potential gas hydrate-existing area and a gas hydrate bearing core. Geochemical analysis suggests that there is an ongoing gas hydrate decomposing and AOM process in Core DH_CL_11. In Core GMGS2-16, ancient AOM processes are suggested to dominate its diagenetic process and the gas hydrate there is supposed to be still active. The predominant groups of the microbial communities in the DH_CL_11 are consistent with those in the near surface layer of GMGS2-16 as well as other known gas hydrate-bearing sites, suggesting a high possibility for the existing of gas hydrate underlying Core DH_CL_11. Overall, integrated geochemical and microbiological analyses are informative in characterizing sediments from gas hydrate-associated areas in the South China Sea.

Acknowledgements

The authors are grateful to Yang Shengxiong, Zhang Guangxue, and Liang Jinqiang from the Guangzhou Marine Geological Survey for providing samples and valuable suggestions. Special appreciation is extended to staffs from the School of Life Sciences in the Sun Yat-sen University. They also acknowledge the editor and reviewers.

References

Berner R A. 1982. Burial of organic carbon and pyrite sulfur in the modern ocean; its geochemical and environmental significance. American Journal of Science, 282(4): 451–473

Bhatnagar G, Chapman W G, Dickens G R, et al. 2008. Sulfate-methane transition as a proxy for average methane hydrate saturation in marine sediments. Geophysical Research Letters, 35(3): L03611

Bi Haibo. 2010. Amount estimation and geochemical analysis of gas hydrate of Taixinan Basin (in Chinese)[dissertation]. Qingdao: Institute of Oceanology, Chinese Academy of Sciences

Boetius A, Ravenschlag K, Schubert C J, et al. 2000. A marine microbial consortium apparently mediating anaerobic oxidation of methane. Nature, 407(6804): 623–626

Boetius A, Suess E. 2004. Hydrate Ridge: a natural laboratory for the study of microbial life fueled by methane from near-surface gas hydrates. Chemical Geology, 205(3–4): 291–310

Borowski W S, Paull C K, Ussler III W. 1996. Marine pore-water sulfate profiles indicate in situ methane flux from underlying gas hydrate. Geology, 24(7): 655–658

Borowski W S, Paull C K, Ussler III W. 1999. Global and local variations of interstitial sulfate gradients in deep-water, continental margin sediments: sensitivity to underlying methane and gas hydrates. Marine Geology, 159(1–4): 131–154

Briggs B R, Graw M, Brodie E L, et al. 2013. Microbial distributions detected by an oligonucleotide microarray across geochemical zones associated with methane in marine sediments from the Ulleung Basin. Marine and Petroleum Geology, 47: 147–154

Briggs B R, Inagaki F, Morono Y, et al. 2012. Bacterial dominance in subseafloor sediments characterized by methane hydrates. FEMS Microbiology Ecology, 81(1): 88–98

Campbell K A. 2006. Hydrocarbon seep and hydrothermal vent paleoenvironments and paleontology: past developments and future research directions. Palaeogeography, Palaeoclimatology, Palaeoecology, 232(2–4): 362–407

Chen Fang, Lu Hongfeng, Liu Jian, et al. 2016. Sedimentary geochemical response to gas hydrate episodic release on the northeastern slope of the South China Sea. Earth Science (in Chinese), 41(10): 1619–1629

Chen Fang, Su Xin, Nurnberg D, et al. 2006. Lithologic features of sediments characterized by high sedimentation rates since the last glacial maximum from Dongsha area of the South China Sea. Marine Geology & Quaternary Geology (in Chinese), 26(6): 9–17

Dählmann A, de Lange G J. 2003. Fluid-sediment interactions at Eastern Mediterranean mud volcanoes: a stable isotope study from ODP Leg 160. Earth and Planetary Science Letters, 212(3-4): 377–391

Dickens G R. 2001. Sulfate profiles and barium fronts in sediment on the Blake Ridge: present and past methane fluxes through a large gas hydrate reservoir. Geochimica et Cosmochimica Acta, 65(4): 529–543

Ding Weiwei, Wang Yuming, Chen Hanlin, et al. 2004. Deformation characters and its tectonic evolution of the Southwest Taiwan Basin. Journal of Zhejiang University (Science Edition) (in Chinese), 31(2): 216–220

Freire A F M, Matsumoto R, Akiba F. 2012. Geochemical analysis as a complementary tool to estimate the uplift of sediments caused by shallow gas hydrates in mounds at the seafloor of Joetsu basin, eastern margin of the Japan Sea. Journal of Geological Research, 2012: 839840

Goldhaber M B. 2003. Sulfur-rich sediments. In: Mackenzie F T, ed. Sediments, Diagenesis, and Sedimentary Rocks. Amsterdam: Elsevier, 257–288

Gong Junli, Sun Xiaoming, Lu Hongfeng. 2014. Physical and geochemical analysis of site DH_CL_11: implications for the presence of gas hydrate deposit in SW Taiwan. Acta Geologica Sinica, 88(S2): 1235–1236

Han Xiqiu, Suess E, Huang Yongyang, et al. 2008. Jiulong methane reef: microbial mediation of seep carbonates in the South China Sea. Marine Geology, 249(3–4): 243–256

Han Xiqiu, Suess E, Liebetrau V, et al. 2014. Past methane release events and environmental conditions at the upper continental slope of the South China Sea: constraints by seep carbonates. International Journal of Earth Sciences, 103(7): 1873–1887

Han Xiqiu, Yang Kehong, Huang Yongyang. 2013. Origin and nature of cold seep in northeastern Dongsha area, South China Sea: evidence from chimney-like seep carbonates. Chinese Science Bulletin, 58(30): 3689–3697

Harrison B K, Zhang Husen, Berelson W, et al. 2009. Variations in archaeal and bacterial diversity associated with the sulfate-methane transition zone in continental margin sediments (Santa Barbara Basin, California). Applied and Environmental Microbiology, 75(6): 1487–1499

He Jiaxiong, Xia Bin, Wang Zhixin, et al. 2006. Petroleum geologic characteristics and exploration base of Taixinan Basin in eastern area of continental shelf in northern of the South China Sea. Natural Gas Geoscience (in Chinese), 17(3): 345–350

Helz G R, Bura-Nakić E, Mikac N, et al. 2011. New model for molybdenum behavior in euxinic waters. Chemical Geology, 284(3–4): 323–332

Helz G R, Miller C V, Charnock J M, et al. 1996. Mechanism of molybdenum removal from the sea and its concentration in black shales: EXAFS evidence. Geochimica et Cosmochimica Acta, 60(19): 3631–3642

Hesse R. 2003. Pore water anomalies of submarine gas-hydrate zones as tool to assess hydrate abundance and distribution in the subsurface: what have we learned in the past decade? Earth-Science Reviews, 61(1–2): 149–179

Hu Yu, Feng Dong, Liang Qianyong, et al. 2015. Impact of anaerobic oxidation of methane on the geochemical cycle of redox-sensitive elements at cold-seep sites of the northern South China Sea. Deep Sea Research Part II: Topical Studies in Oceanography, 122: 84–94

Hu Yu, Feng Dong, Peckmann J, et al. 2014. New insights into cerium anomalies and mechanisms of trace metal enrichment in authigenic carbonate from hydrocarbon seeps. Chemical Geology, 381: 55–66

Inagaki F, Nunoura T, Nakagawa S, et al. 2006. Biogeographical distribution and diversity of microbes in methane hydrate-bearing deep marine sediments on the Pacific Ocean Margin. Proceedings of the National Academy of Sciences of the United States of America, 103(8): 2815–2820

Inagaki F, Suzuki M, Takai K, et al. 2003a. Microbial communities associated with geological horizons in coastal subseafloor sediments from the Sea of Okhotsk. Applied and Environmental Microbiology, 69(12): 7224–7235

Inagaki F, Takai K, Kobayashi H, et al. 2003b. *Sulfurimonas autotrophica* gen. nov., sp. nov., a novel sulfur-oxidizing ε-proteobacterium isolated from hydrothermal sediments in the Mid-Okinawa Trough. International Journal of Systematic and Evolutionary Microbiology, 53(6): 1801–1805

Jiang Hongchen, Dong Hailiang, Ji Shanshan, et al. 2007. Microbial diversity in the deep marine sediments from the Qiongdongnan basin in South China Sea. Geomicrobiology Journal, 24(6): 505–517

Jiao Lu, Su Xin, Wang Yuanyuan, et al. 2015. Microbial diversity in the hydrate-containing and-free surface sediments in the Shenhu area, South China Sea. Geoscience Frontiers, 6(4): 627–633

Johnson J E, Phillips S C, Torres M E, et al. 2014. Influence of total organic carbon deposition on the inventory of gas hydrate in the Indian continental margins. Marine and Petroleum Geology, 58: 406–424

Jørgensen B B, Böttcher M E, Lüschen H, et al. 2004. Anaerobic methane oxidation and a deep H_2S sink generate isotopically heavy sulfides in Black Sea sediments. Geochimica et Cosmochimica Acta, 68(9): 2095–2118

Kampmann K, Ratering S, Kramer I, et al. 2012. Unexpected stability of *Bacteroidetes* and *Firmicutes* communities in laboratory biogas reactors fed with different defined substrates. Applied and Environmental Microbiology, 78(7): 2106–2119

Klauda J B, Sandler S I. 2005. Global distribution of methane hydrate in ocean sediment. Energy & Fuels, 19(2): 459–470

Knittel K, Boetius A. 2009. Anaerobic oxidation of methane: progress with an unknown process. Annual Review of Microbiology, 63(1): 311–334

Kvenvolden K A. 1993. Gas hydrates—geological perspective and global change. Reviews of Geophysics, 31(2): 173–187

Kvenvolden K A. 1988. Methane hydrate—a major reservoir of carbon in the shallow geosphere?. Chemical Geology, 71(1–3): 41–51

Kvenvolden K A, Kastner M. 1990. Gas hydrate of the Peruvian outer continental margin. In: Suess E, Huene R V, Emeis K C, et al., eds. Peru Continental Margin. Proceedings ODP Scientific Results, 112. College Station, TX: Ocean Drilling Program, 517–526

Lanoil B D, La Duc M T, Wright M, et al. 2005. Archaeal diversity in ODP legacy borehole 892b and associated seawater and sediments of the Cascadia Margin. FEMS Microbiology Ecology, 54(2): 167–177

Lee J W, Kwon K K, Azizi A, et al. 2013. Microbial community structures of methane hydrate-bearing sediments in the Ulleung Basin, East Sea of Korea. Marine and Petroleum Geology, 47: 136–146

Li Dongmei, Midgley D J, Ross J P, et al. 2012. Microbial biodiversity in a Malaysian oil field and a systematic comparison with oil reservoirs worldwide. Archives of Microbiology, 194(6): 513–523

Li Lun, Lei Xinhua, Zhang Xin, et al. 2013. Gas hydrate and associated free gas in the Dongsha Area of northern South China Sea. Marine and Petroleum Geology, 39(1): 92–101

Li Tao, Wang Peng, Wang Pinxian. 2008a. Bacterial and archaeal diversity in surface sediment from the south slope of the South China Sea. Acta Microbiologica Sinica (in Chinese), 48(3): 323–329

Li Tao, Wang Peng, Wang Pinxian. 2008b. Microbial diversity in surface sediments of the Xisha Trough, the South China Sea. Acta Ecologica Sinica, 28(3): 1166–1173

Liao Li, Xu Xuewei, Wang Chunsheng, et al. 2009. Bacterial and archaeal communities in the surface sediment from the northern slope of the South China Sea. Journal of Zhejiang University Science B, 10(12): 890–901

Lin Zhiyong, Sun Xiaoming, Lu Yang, et al. 2016a. Stable isotope patterns of coexisting pyrite and gypsum indicating variable methane flow at a seep site of the Shenhu area, South China Sea. Journal of Asian Earth Sciences, 123: 213–223

Lin Zhiyong, Sun Xiaoming, Lu Yang, et al. 2017. The enrichment of heavy iron isotopes in authigenic pyrite as a possible indicator of sulfate-driven anaerobic oxidation of methane: insights from the South China Sea. Chemical Geology, 449: 15–29

Lin Zhiyong, Sun Xiaoming, Peckmann J, et al. 2016b. How sulfate-driven anaerobic oxidation of methane affects the sulfur isotopic composition of pyrite: a SIMS study from the South China Sea. Chemical Geology, 440: 26–41

Lu Hailong, Seo Y T, Lee J W, et al. 2007. Complex gas hydrate from the Cascadia margin. Nature, 445(7125): 303–306

Lu Hongfeng, Chen Fang, Liu Jian, et al. 2006. Characteristics of authigenic carbonate chimneys in Shenhu area, northern South China Sea: recorders of hydrocarbon-enriched fluid activity. Geological Review (in Chinese), 52(3): 352–357

Lu Hongfeng, Liu Jian, Chen Fang, et al. 2005. Mineralogy and stable isotopic composition of authigenic carbonates in bottom sediments in the offshore area of southwest Taiwan, South China Sea: evidence for gas hydrates occurrence. Earth Science Frontier (in Chinese), 12(3): 268–276

Lu Hongfeng, Sun Xiaoming, Zhang Mei. 2011. Mineralogy and Geochemistry of the Authigenic Sediments of Gas Hydrate in the South China Sea (in Chinese). Beijing: Science Press

Lu Yang, Sun Xiaoming, Lin Zhiyong, et al. 2015. Cold seep status archived in authigenic carbonates: mineralogical and isotopic evidence from northern South China Sea. Deep Sea Research Part II: Topical Studies in Oceanography, 122: 95–105

Marchesi J R, Weightman A J, Cragg B A, et al. 2001. Methanogen and bacterial diversity and distribution in deep gas hydrate sediments from the Cascadia Margin as revealed by 16S rRNA molecular analysis. FEMS Microbiology Ecology, 34(3): 221–228

McDonnell S L, Max M D, Cherkis N Z, et al. 2000. Tectono-sedimentary controls on the likelihood of gas hydrate occurrence near Taiwan. Marine and Petroleum Geology, 17(8): 929–936

McManus J, Berelson W M, Severmann S, et al. 2006. Molybdenum and uranium geochemistry in continental margin sediments: paleoproxy potential. Geochimica et Cosmochimica Acta, 70(18): 4643–4662

Mills H J, Hodges C, Wilson K, et al. 2003. Microbial diversity in sediments associated with surface-breaching gas hydrate mounds in the Gulf of Mexico. FEMS Microbiology Ecology, 46(1): 39–52

Nauhaus K, Treude T, Boetius A, et al. 2005. Environmental regulation of the anaerobic oxidation of methane: a comparison of ANME-I and ANME-II communities. Environmental Microbiology, 7(1): 98–106

Niewöhner C, Hensen C, Kasten S, et al. 1998. Deep sulfate reduction completely mediated by anaerobic methane oxidation in sediments of the upwelling area off Namibia. Geochimica et Cosmochimica Acta, 62(3): 455–464

Nunoura T, Takaki Y, Kazama H, et al. 2012. Microbial diversity in deep-sea methane seep sediments presented by SSU rRNA gene tag sequencing. Microbes and Environments, 27(4): 382–390

Orcutt B N, Joye S B, Kleindienst S, et al. 2010. Impact of natural oil and higher hydrocarbons on microbial diversity, distribution, and activity in Gulf of Mexico cold-seep sediments. Deep Sea Research Part II: Topical Studies in Oceanography, 57(21-23):

2008–2021
Parkes R J, Cragg B, Roussel E, et al. 2014. A review of prokaryotic populations and processes in sub-seafloor sediments, including biosphere: geosphere interactions. Marine Geology, 352: 409–425
Penner T J, Foght J M, Budwill K. 2010. Microbial diversity of western Canadian subsurface coal beds and methanogenic coal enrichment cultures. International Journal of Coal Geology, 82(1–2): 81–93
Pierre C, Rouchy J M, Gaudichet A. 2000. Diagenesis in the gas hydrate sediments of the Blake Ridge: mineralogy and stable isotope compositions of the carbonate and sulfide minerals. In: Paull C K, Matsumoto R, Wallace P J, et al., eds. Proceedings of the Ocean Drilling Program, Scientific Results, Volume 164. College Station, TX: Ocean Drilling Program, 139–146
Polymenakou P N, Mandalakis M. 2013. Assessing the short-term variability of bacterial composition in background aerosols of the Eastern Mediterranean during a rapid change of meteorological conditions. Aerobiologia, 29(3): 429–441
Reeburgh W S. 2007. Oceanic methane biogeochemistry. Chemical Reviews, 107(2): 486–513
Reed D W, Fujita Y, Delwiche M E, et al. 2002. Microbial communities from methane hydrate-bearing deep marine sediments in a Forearc basin. Applied and Environmental Microbiology, 68(8): 3759–3770
Rice P, Longden I, Bleasby A. 2000. EMBOSS: the European molecular biology open software suite. Trends in Genetics, 16(6): 276–277
Sato H, Hayashi K, Ogawa Y, et al. 2012. Geochemistry of deep sea sediments at cold seep sites in the Nankai Trough: insights into the effect of anaerobic oxidation of methane. Marine Geology, 323-325: 47–55
Schleifer K H, Kraus J, Dvorak C, et al. 1985. Transfer of *Streptococcus lactis* and related streptococci to the genus *Lactococcus* gen. nov. Systematic and Applied Microbiology, 6(2): 183–195
Shyu C T, Chen Y J, Chiang S T, et al. 2006. Heat flow measurements over bottom simulating reflectors, offshore southwestern Taiwan. Terrestrial, Atmospheric and Oceanic Sciences, 17(4): 845–869
Shyu C T, Hsu S K, Liu C S. 1998. Heat flows off southwest Taiwan: measurements over mud diapirs and estimated from bottom simulating reflectors. Terrestrial, Atmospheric and Oceanic Sciences, 9(4): 795–812
Snyder G T, Hiruta A, Matsumoto R, et al. 2007. Pore water profiles and authigenic mineralization in shallow marine sediments above the methane-charged system on Umitaka Spur, Japan Sea. Deep Sea Research Part II: Topical Studies in Oceanography, 54(11–13): 1216–1239
Song Haibin, Geng Jianhua. Wang Howking, et al 2001. A preliminary study of gas hydrates in Dongsha region north of South China Sea. Chinese Journal of Geophysics, 44(5): 687–695
Stackebrandt E, Goebel B M. 1994. Taxonomic note: a place for DNA-DNA reassociation and 16S rRNA sequence analysis in the present species definition in bacteriology. International Journal of Systematic and Evolutionary Microbiology, 44(4): 846–849
Sun Qiliang, Wu Shiguo, Cartwright J, et al. 2012. Shallow gas and focused fluid flow systems in the Pearl River Mouth Basin, northern South China Sea. Marine Geology, 315-318: 1–14
Takeuchi R, Machiyama H, Matsumoto R. 2002. Methane seep, chemosynthetic communities, and carbonate crusts on the Kuroshima Knoll, offshore Ryukyu islands. AAPG Annual Meeting, Houston, Texas
Tang Yueqin, Shigematsu T, Morimura S, et al. 2005. Microbial community analysis of mesophilic anaerobic protein degradation process using bovine serum albumin (BSA)-fed continuous cultivation. Journal of Bioscience and Bioengineering, 99(2): 150–164
Tourova T P, Spiridonova E M, Berg I A, et al. 2007. Phylogeny and evolution of the family *Ectothiorhodospiraceae* based on comparison of 16S rRNA, *cbbL* and *nifH* gene sequences. International Journal of Systematic and Evolutionary Microbiology, 57(10): 2387–2398
Tréhu A M, Long P E, Torres M E, et al. 2004. Three-dimensional distribution of gas hydrate beneath southern Hydrate Ridge: constraints from ODP Leg 204. Earth and Planetary Science Letters, 222(3–4): 845–862
Wang Jiasheng, Suess E. 2002. Indicators of δ^{13}C and δ^{18}O of gas hydrate-associated sediments. Chinese Science Bulletin, 47(19): 1659–1663
Waseda A. 1988. Organic carbon content, bacterial methanogenesis, and accumulation processes of gas hydrates in marine sediments. Geochemical Journal, 32(3): 143–157
Wu Lushan, Yang Shengxiong, Liang Jinqiang, et al. 2013. Variations of pore water sulfate gradients in sediments as indicator for underlying gas hydrate in Shenhu Area, the South China Sea. Science China: Earth Sciences, 56(4): 530–540
Wu Shiguo, Zhang Guangxue, Huang Yongyang, et al. 2005. Gas hydrate occurrence on the continental slope of the northern South China Sea. Marine and Petroleum Geology, 22(3): 403–412
Yamane K, Hattori Y, Ohtagaki H, et al. 2011. Microbial diversity with dominance of 16S rRNA gene sequences with high GC contents at 74 and 98°C subsurface crude oil deposits in Japan. FEMS Microbiology Ecology, 76(2): 220–235
Yan Tingfen, Ye Qi, Zhou Jizhong, et al. 2006. Diversity of functional genes for methanotrophs in sediments associated with gas hydrates and hydrocarbon seeps in the Gulf of Mexico. FEMS Microbiology Ecology, 57(2): 251–259
Yanagawa K, Kouduka M, Nakamura Y, et al. 2014. Distinct microbial communities thriving in gas hydrate-associated sediments from the eastern Japan Sea. Journal of Asian Earth Sciences, 90: 243–249
Yang Tao, Jiang Shaoyong, Ge Lu, et al. 2010. Geochemical characteristics of pore water in shallow sediments from Shenhu area of South China Sea and their significance for gas hydrate occurrence. Chinese Science Bulletin, 55(8): 752–760
Yang Tao, Jiang Shaoyong, Yang Jinghong, et al. 2008. Dissolved inorganic carbon (DIC) and its carbon isotopic composition in sediment pore waters from the Shenhu area, northern South China Sea. Journal of Oceanography, 64(2): 303–310
Ye Hong, Yang Tao, Zhu Guorong, et al. 2016. Pore water geochemistry in shallow sediments from the northeastern continental slope of the South China Sea. Marine and Petroleum Geology, 75: 68–82
Yin Xijie, Chen Jian, Guo Yingying, et al. 2011. Sulfate reduction and methane anaerobic oxidation: isotope geochemical evidence from the pore water of coastal sediments in the Jiulong Estuary. Haiyang Xuebao (in Chinese), 33(4): 121–128
Zhang Bidong, Wu Daidai, Wu Nengyou. 2015. Characteristics of sedimentary geochemistry and their responses to cold-seep activities in Dongsha, the northern South China Sea. Marine Geology Frontiers (in Chinese), 31(9): 14–27
Zhang Guangxue, Liang Jinqiang, Lu Jing'an, et al. 2014a. Characteristics of natural gas hydrate reservoirs on the northeastern slope of the South China Sea. Natural Gas Industry (in Chinese), 34(11): 1–10
Zhang Mei, Konishi H, Xu Huifang, et al. 2014b. Morphology and formation mechanism of pyrite induced by the anaerobic oxidation of methane from the continental slope of the NE South China Sea. Journal of Asian Earth Sciences, 92: 293–301
Zhang Yong, Su Xin, Chen Fang, et al. 2012. Microbial diversity in cold seep sediments from the northern South China Sea. Geoscience Frontiers, 3(3): 301–316
Zheng Yan, Anderson R F, Alexander van G, et al. 2000. Authigenic molybdenum formation in marine sediments: a link to pore water sulfide in the Santa Barbara Basin. Geochimica et Cosmochimica Acta, 64(24): 4165–4178
Zheng Yan, Anderson R F, Alexander van G, et al. 2002. Remobilization of authigenic uranium in marine sediments by bioturbation. Geochimica et Cosmochimica Acta, 66(10): 1759–1772
Zhuang Chang, Chen Fang, Cheng Sihai, et al. 2016. Light carbon isotope events of foraminifera attributed to methane release from gas hydrates on the continental slope, northeastern South China Sea. Science China: Earth Sciences, 59(10): 1981–1995